REPORT DOCUMENTATION PAGE

Form Approved
OMB No. 0704-0188

1. REPORT DATE *(DD-MM-YYYY)*	**2. REPORT TYPE**	**3. DATES COVERED** *(From - To)*
29-03-2007	Technical Paper and Briefing Charts	

4. TITLE AND SUBTITLE

Laser Induced Breakdown Spectroscopy (LIBS) Applied to Reacting Gases for Mixture Ratio Measurement and Detection of Metallic Species

5a. CONTRACT NUMBER
FA9300-06-C-1002

5b. GRANT NUMBER

5c. PROGRAM ELEMENT NUMBER

6. AUTHOR(S)
Matthew Thomas, Stelu Deaconu, James Lewis and Edward Coy

5d. PROJECT NUMBER
300506JN

5e. TASK NUMBER

5f. WORK UNIT NUMBER

7. PERFORMING ORGANIZATION NAME(S) AND ADDRESS(ES)

CFD Research Corporation
215 Wynn Drive
Huntsville AL 35805

8. PERFORMING ORGANIZATION REPORT NUMBER

AFRL-PR-ED-TP-2007-170

9. SPONSORING / MONITORING AGENCY NAME(S) AND ADDRESS(ES)

Air Force Research Laboratory (AFMC)
AFRL/PRS
5 Pollux Drive
Edwards AFB CA 93524-7048

10. SPONSOR/MONITOR'S ACRONYM(S)

11. SPONSOR/MONITOR'S NUMBER(S)
AFRL-PR-ED-TP-2007-170

12. DISTRIBUTION / AVAILABILITY STATEMENT

Distribution A: Approved for public release; distribution unlimited. (Public Affairs No. 07123A).

13. SUPPLEMENTARY NOTES
Presented at the JANNAF 54th Propulsion Meeting/3rd Liquid Propulsion Subcommittee/2nd Spacecraft Propulsion Subcommittee/5th Modeling and Simulation Subcommittee Joint Meeting, Denver, CO, 14-17 May 2007.

14. ABSTRACT

Measurements of LIBS spectra in an atmospheric pressure laboratory burner and pressurized sub-scale rocket combustion chamber are reported. LIBS is being developed as diagnostic for near wall measurements in liquid rocket combustion chambers as part of an AFRL effort to experimentally determine relative concentrations of major combustion species in rocket chambers and reduce validation uncertainty of CFD heat transfer tools. The potential for simultaneous use as a health-monitoring diagnostic i.e. detection of wall and injector erosion is also discussed.

15. SUBJECT TERMS

16. SECURITY CLASSIFICATION OF:			**17. LIMITATION OF ABSTRACT**	**18. NUMBER OF PAGES**	**19a. NAME OF RESPONSIBLE PERSON**
					Dr. Edward B. Coy
a. REPORT	**b. ABSTRACT**	**c. THIS PAGE**	SAR	30	**19b. TELEPHONE NUMBER** *(include area code)*
Unclassified	**Unclassified**	**Unclassified**			N/A

Standard Form 298 (Rev. 8-98)
Prescribed by ANSI Std. 239.18

Laser Induced Breakdown Spectroscopy (LIBS) Applied to Reacting Gases for Mixture Ratio Measurement and Detection of Metallic Species

Matthew Thomas[1], Stelu Deaconu[1], James Lewis[2], Edward Coy[3]
1 CFD Research Corp., Huntsville, AL
2 University of Tennessee Space Institute
3 Air Force Research Laboratory

Abstract
Measurements of LIBS spectra in an atmospheric pressure laboratory burner and pressurized sub-scale rocket combustion chamber are reported. LIBS is being developed as diagnostic for near wall measurements in liquid rocket combustion chambers as part of an AFRL effort to experimentally determine relative concentrations of major combustion species in rocket chambers and reduce validation uncertainty of CFD heat transfer tools. The potential for simultaneous use as a health-monitoring diagnostic i.e. detection of wall and injector erosion is also discussed.

Introduction
Laser Induced Breakdown Spectroscopy (LIBS) is an optical diagnostic technique capable of providing an analysis of the local concentration of various atomic species including C and O, H and metallic species in a test media. Generally, LIBS uses a single or double pulse laser beam to produce a plasma within the focal region that includes the test point, and is applicable to single-, two-, and multi-phase media, see for instance Fisher et al, (2001), Anglos et al, (1997) and Hohreiter and Hahn, (2005). Some LIBS applications require the use of the lowest power, highest irradiance source that will provide predictable breakdown events, which makes necessary an accurate characterization of the stochastic nature of the breakdown. Other applications require detailed understanding of the spatial and temporal features of the pulsed laser-produced plasma for accurate descriptions of plasma chemistry and gas dynamic phenomena. The energy deposited in the plasma by the laser beam atomizes, in the strict meaning, the target media and creates electronically excited species in the test volume. In the subsequent spectroscopic observation of ionized and neutral atomic species, the spectral signature of the radiating species defines the constituents, and the corresponding signal levels yield a measure of the concentration or density of each observed constituent, Fang et al. (2002).

The application of LIBS to the determination of the equivalence ratio in a combustion environment has been attempted in laboratory environments for low-pressure acetylene flames, Sandrowitz et al. (1998) atmospheric pressure methane-air jet diffusion flames, Phuoc and White, (1999) and within spark ignited combustion engines, Ferioli et al., (2003), but to date no LIBS diagnosis of rocket combustion has been reported for high temperature and pressure rocket combustion. This paper documents the efforts undertaken in this direction by CFD Research Corp. and the University of Tennessee Space Institute.

The atomic emission lines recorded in LIBS are characterized by wavelength, amplitude, and width. While the line wavelength is solely determined by the nature of the emitting

species and is responsible for the good qualitative species discrimination of LIBS, the relationship between the line amplitude/width and species concentration is not straightforward. Other factors contributing to line amplitude/width are gas temperature (e.g. by thermal Doppler line broadening) and optical properties (e.g. absorption) within the plasma. A relationship between these parameters, laser power, plasma properties, and the shape of the emission lines must thus be established to determine species concentrations.

Energy Absorption in Laser-Induced Breakdown

Significant energy absorption of a cascade type after optical breakdown starts with the generation of the initial free electrons. Following the rapid growth of the electron density, the initial plasma becomes optically thick and absorbs practically all of the incident energy in the latter portion of the laser pulse. The temporal structure of energy absorption process in LIBS is described by Chen et al. (2000), Plemmons (1996), Chen (1998) and Dors (2000). The threshold value of optical breakdown is defined as the laser power at which one-half of the incident laser pulses induce significant energy absorption and cause breakdown. Since the energy absorption process begins only when the laser power (or specifically, the irradiance) reaches this threshold range, the leading edge of the pulse below threshold is transmitted unperturbed into and through the focal zone. When the laser peak-power is near the threshold value the uncertainty of absorption energy is very large, and the difference of initiation time between breakdowns can be as long as 3 ns. For higher incident laser power, the absorption starts earlier, and the process lasts longer, the fraction of absorbed energy increases and the fractional deviation of absorption energy reduces significantly. Figure 1 shows the experimental results of the incident laser-energies of thousands of pulses and the corresponding transmitted energies.

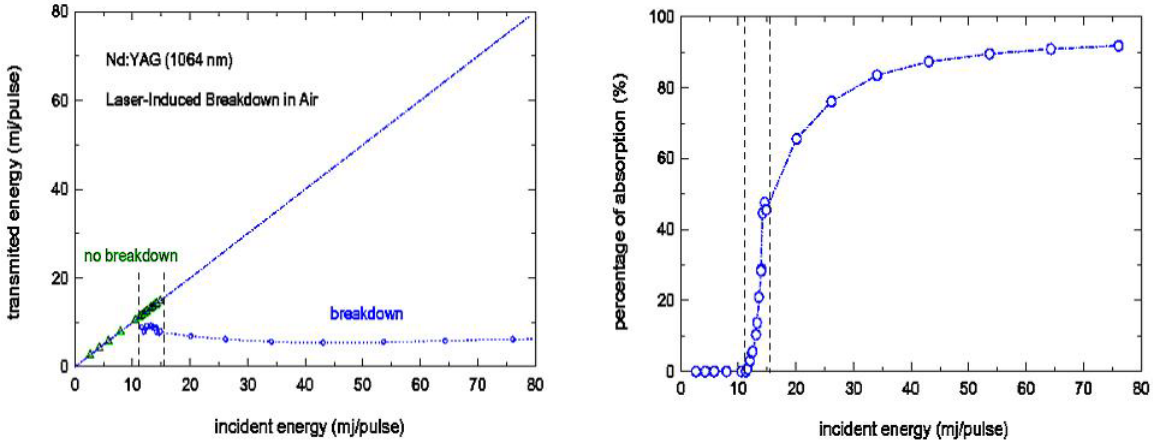

Figure 1. Energy-absorption study in laser-induced air breakdown (from Chen et al. (2000))

Since significant scattering and diffracted light were not observed in the UTSI experiments, the absorbed energies for the breakdowns are equal to the difference of incident and transmitted energies. For these graphs, each plotted point, which corresponds to a fixed incident laser-energy (±1%), is the statistical result of the recording of more than 100 pulses. The error-bars show the deviations of these one

hundred-plus pulses. In Figure 1(left), three energy regions with quite different characteristics can be seen. For the laser pulse energy less than 11 mJ, no breakdown occurred. The entire incident pulse-energy transmits through the focal zone, and the data points all lie on the dash-dot line (with slope equal to1), corresponding to the situation that no absorption or breakdown occurs). When the incident pulse-energies were larger than 16 mJ, all the laser-pulses caused significant absorption and created breakdowns. For the laser-pulses with energies between 11 and 16 mJ, only a certain fraction of pulses induced breakdowns (symbolized as circles), and the remainder did not (symbolized as triangles). Shown in Figure 1(right) is the percentage absorption as a function of the incident pulse energy. As the result shows, about 50% of incident energy was absorbed when the input laser energy is just above the breakdown threshold range, which implies that, following the initiation of breakdown, the free-electron grows to a highly absorbent density within a short period of time (approximately) 1-2ns. The electron growth rate, which depends on the laser irradiance, is then expected to be much faster than the reciprocal of laser pulse-width of 6.5 ns for a stronger laser excitation.

LIBS Theoretical Analysis

The accuracy of LIBS is dependent on selecting appropriate laser parameters for the application. The obvious advantages of the LIBS technique are that it is highly versatile (it can be used to interrogate solids, liquids and gases), provides localized (sub-millimeter) analysis, is remarkably fast (scans can be performed in seconds or less), and requires little or no sample preparation. However, there is no single LIBS system that will work in all situations. Also, much of the work done (to date) with commercial and even more specialized LIBS systems is qualitative or semi-quantitative and is concerned mostly with the detection of particular compounds without concern for the concentration. This proposed application of LIBS addresses the local, internal engine measurements of the fuel to oxidizer ratio (F/O) for methane and both gaseous and liquid oxygen and the detection and quantification of erosion and degradation products of the engine components. The effort aims are to obtain accurate qualitative LIBS results by taking into consideration both the complexity of the combustion process and the properties of the plasma phenomenon.

A *conversational* description of LIBS is relatively simple. All constituents of the sample are atomized and heated to plasma conditions by the laser-induced breakdown. The entire spectroscopic signal of an atomic species is observed regardless of its original state, chemical bonding, and the species' elemental mass or number density. The interaction of the laser with a gaseous mixture, for example, heats and ionizes a small volume of the sample. The laser beam energy is absorbed by the gas and by the generated plasma, and several phenomena occur which are responsible for reflection of radiation, electron emission, sample heating and phase changes, all affecting the physical properties of the plume in a way characteristic to the sample composition. Once the breakdown and plasma formation has occurred, the thermodynamic state of the plasma sample can be described as local thermal equilibrium (LTE), and the concentration of the density of each atomic species in the various radiating states is proportional to the ground state and total density of that species. Thus, if the plasma is optically thin in a proper temporal and spatial observation window, the spectrally integrated line intensity, I_{α}

corresponding to the transition between levels E_k and E_i (with for instance E_i ground state) of the atomic (carbon or oxygen) species with concentration C_α can be expressed as

$$I_\alpha = \beta \cdot C_\alpha \frac{g_k A_{ki} \cdot \exp(-E_k / k_B T)}{U_\alpha(T)}, \qquad \text{Eqn. 1.1}$$

where T is the plasma temperature, U_α (T) is the partition function, k_B is the Boltzmann constant, and β is a constant depending on experimental conditions. Assuming only small variation of plasma temperature and concentration, all factors in Eqn. 1 are in common except for concentration and line intensity for each element. This allows a simple linear relationship to be established between the specific line intensity and the relevant elemental concentration. Moreover, by noting that the integrated line intensity of Eqn. 1 depends linearly (through the constant C_α) on the plasma density, it can be concluded that an increase of the accuracy in element concentration measurements can be obtained by using a reference sample with thermal properties similar to those of the unknown sample. In this case, including the plasma temperature in the quantitative analysis allows for an improvement in the overall experimental accuracy. By rationing the line intensities originated from the sample and by a reference material (with known elemental concentration), at temperatures T_α and T_r, respectively, we obtain from Eqn. 1.1

$$\frac{I_\alpha(T_\alpha)}{I_r(T_r)} = \frac{C_\alpha}{C_r} \cdot \frac{\exp(-E_k / k_B (1/T_\alpha - 1/T_r))}{U_\alpha(T_\alpha)/U_r(T_r)} \qquad \text{Eqn. 1.2}$$

Eqn. 1.2 allows the evaluation of C_α from the measured LIBS line intensity, while the other parameters are derived from atomic databases at known plasma temperatures. In order to estimate the plasma temperature, we take the natural logarithm of Eqn. 1.1 and obtain

$$\ln\left(\frac{I_\alpha}{g_k \cdot A_{ki}}\right) = -\frac{E_k}{k_B \cdot T} + \ln\left(\frac{C_\alpha \cdot \beta}{U_\alpha(T_\alpha)}\right), \qquad \text{Eqn. 1.3}$$

In the typical Boltzman plot where the ordinate is identified by the left hand term of Eqn. 1.3 and the abscissa by E_k, different emission lines intensities belonging to the same element in the spectrum lie along a straight line with a slope of $1/k_B T$. If sample and reference experimental data are available for each element in the sample, the combined use of Eqn. 1.2 and Eqn. 1.3 allows for the evaluation of species concentration.

Alternatively, if calibration data at specific temperatures are not available for certain species of interest, wavelength and spontaneous emission signal level calibrations can be performed in-situ to provide the desired density. This level of description then proceeds from the predictive relations of equilibrium compositions provided by the Saha equation:

$$\frac{n_i + n_e}{n_i} = \frac{2}{\Lambda^3} \cdot \frac{g_{i+1}}{g_i} \exp\left[-\frac{(\varepsilon_{i+1} - \varepsilon_i)}{k_B T}\right] \qquad \text{Eqn. 1.4}$$

where: n_i is the density of atoms in the i^{-th} state of ionization, that is with i electrons removed, g_i is the degeneracy of states for the i-ions, $\in_i$ is the energy required to remove

an electron from an (i-1)-level ion, creating an i-level ion, n_e is the electron density. Here Λ, is the thermal de Broglie wavelength of an electron:

$$\Lambda \cong \sqrt{\frac{h^2}{2\pi \cdot m_e k_B T}} \qquad \text{Eqn. 1.5}$$

where m_e is the mass of an electron, T is the temperature of the plasma, and h is Planck's constant. Using the spontaneous emission equation,

$$n(t) = n_0 \cdot e^{-t \cdot A_{21}} \qquad \text{Eqn. 1.6}$$

where n_0 is the initial number of atoms in the excited state, t is time and A is the reciprocal lifetime of the assumed two level atom, the plasma temperature can be determined by matching the experimental spectra (within a certain wavelength range) with the blackbody spectrum

$$I(\upsilon) = \frac{2h\upsilon^3}{c^2} \cdot \frac{1}{\exp(h\upsilon / kT) - 1} \qquad \text{Eqn. 1.7}$$

where I(ν) is the radiation intensity, or spectral radiance, ν = c/λ, c is the speed of light, and T is the plasma temperature. With plasma density and plasma temperature thus determined, the concentration of the species can be determined from individual line intensity, I_{ij} corresponding to the transition between levels E_i and E_j of the atomic (e.g. carbon, oxygen, Cr, Fe, etc.) species using a relationship similar to Eqn. 1.1.

$$I_{ij} = \alpha \cdot N_k \cdot A_{ij} \cdot \exp(-\Delta E_{ij} / k_B T) \qquad \text{Eqn. 1.8}$$

The approach employed in this program is a modification of the typical analytical laboratory technique of a steady-state plasma source. In this work, specific atomic lines are selected for measurement at detection times that are optimal for the laser and detector, and pre-test calibrations are performed to obtain the desired quantitative results.

Experimental Apparatus

Data for methane and oxygen were collected at UTSI within a laboratory setting for a flat flame, McKenna, burner and a CFDRC test rocket motor. The tests were conducted using a well-characterized 1064nm Nd:YAG laser beam that has been used in previous laser-induced plasma and ignition studies. In these preliminary measurements we have not removed the laser's doubling crystal that produces 532nm output if desired, and as a result, we have not used the maximum output available from the laser at 1064nm. However, although the laser energy for these data is well below the normal 100mJ per pulse that is typical, the pulse energy far exceeds breakdown threshold, which is required to ensure stable LIBS data. The detection system for this work consisted of a F/6 fiber optics collector of 3-m length that transmits the collected signal to the Acton SP500 spectrometer. The detector system was a linear array of 1024 silicon diodes behind a gated image intensifier. The experimental setup used for these experiments, is similar to that described in greater detail by Chen et. al. (2000) and is shown in Figure 2.

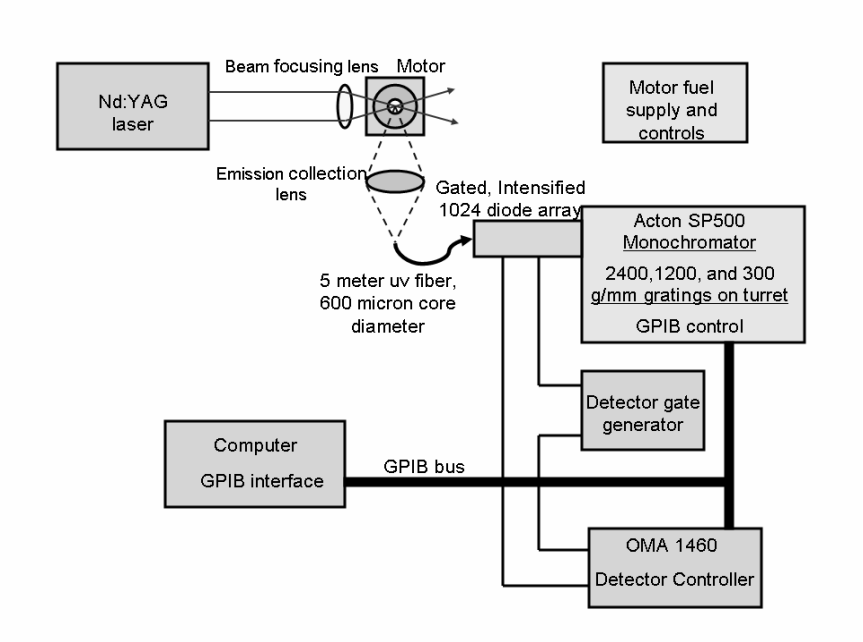

Figure 2. Schematics of LIBS Detection System

Data were obtained for atomic species lines observed in pure methane, pure oxygen, and for several mixtures of methane and oxygen with a McKenna flat flame burner and within CFDRC laboratory scale rocket motor, see Figure 3. The gas flow was metered using the McKenna burner apparatus and using the matched shroud flow, our previous computations using the CFD-ACE+ code and experimental data indicated that we are obtaining results within a spatial region of low radial and axial gradients of the flow.

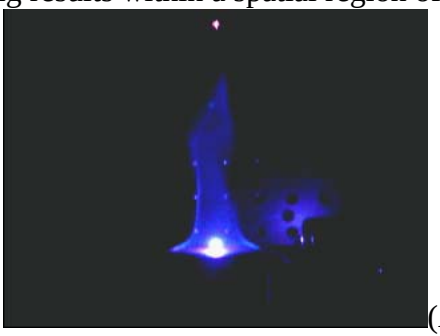
(A)
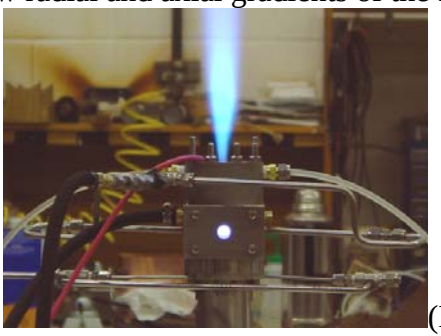
(B)

Figure 3. LIBS with McKenna Flat Flame Burner (A) and CFDRC Rocket Combustion Chamber (B)

Both pure and mixed flows of CH_4 and O_2 have been probed using the optical fiber-coupled OMA detector, and spectral signals have been measured for neutral and ionized atomic carbon and oxygen atoms. A qualitative description of the selection of detection parameters is useful. For a typical gas sample, the nominal 10nsec laser absorption produces a plasma of maximum temperature of 75,000 – 100,000K, depending upon the incident laser beam irradiance. Following the beam absorption, plasma growth and heating, the cooling of the plasma begins, and spectral data indicate clearly these regimes. LTE is assumed to characterize the time regions and spectral features of interest, and previous data can be offered to show this for simple plasma cases. Early times following

laser cessation have the largest T's and the richest ionic spectra, but this region also has the largest background continuum. Therefore, though the signal may be large, the signal-to-background ratio (S/B) can be unacceptably low. As a practical measure then, one wishes to obtain data for high S/B ratios, good signal values and at times such that the wealth of ionic and atomic data have not been depleted by recombination, quenching and plasma T cooling. The preliminary data of Phase I have been used to locate those desired times and spectral regions.

The McKenna Burner Calibration Runs

The gas flow is obtained using the McKenna burner apparatus, and using the matched shroud flow, our previous computations using the CFD-ACE code and experimental data indicate that we are obtaining results within a spatial region of low radial and axial gradients of the flow. Both pure and mixed flows of CH_4 and O_2 have been observed using the optical fiber-coupled OMA detector, and spectral signals have been measured for neutral and ionized atomic carbon and oxygen atoms.

A qualitative description of the selection of detection parameters is useful. For a typical gas sample, the nominal 10nsec laser absorption produces a plasma of maximum temperature of 75,000 – 100,000K, depending upon the incident laser beam irradiance. Following the beam absorption, plasma growth and heating, the cooling of the plasma begins, and spectral data indicate clearly these regimes. LTE is assumed to characterize the time regions and spectral features of interest, and previous data can be offered to show this for simple plasma cases. Early times following laser cessation have the largest T's and the richest ionic spectra, but this region also has the largest background continuum. Therefore, though the signal may be large, the signal-to-background ratio (S/B) can be unacceptably low. As a practical measure then, one wishes to obtain data for high S/B ratios, good signal values and at times such that the wealth of ionic and atomic data have not been depleted by recombination, quenching and plasma T cooling. The preliminary data of Phase I have been used to locate those desired times and spectral regions.

Hydrogen Spectra: A separate and independent measure of the fuel concentration is provided by H-atom LIBS spectra that result from the CH_4 species. The Balmer series of the H-atom spectra is well known and is the result of the sequence of atomic transitions of the change of the principal quantum number $\mathbf{n} \rightarrow 2$, where **n** ranges from 3 to larger numbers.

Hydrogen spectra were obtained using a 0.5 m focal length Acton spectrometer with f/6.9 aperture. The Czerny-Turner mounts include for use three gratings. The spectrometer reciprocal linear dispersion (RLD) of 1.67 nm/mm is obtained using the 1200 groove/mm (g/mm) grating. The Balmer series data shown in Figures 4.A and B were obtained as "survey" spectra using a 150g/mm grating, and the low resolution of the spectra is indicative of the corresponding nominal 13nm/mm RLD. The data show clearly the broad background continuum at the earliest time following the laser breakdown event, and this is typical of electron-ion recombination spectra. For times of 200nsec and greater following breakdown and termination of the laser pulse, the line spectra are well defined and easily measured, and yield additional fuel species data, and it is seen that results are obtained into the microsecond region.

Of more importance, perhaps, is the information provided by the Balmer series concerning the state of the plasma. It is recalled (Eqn. 1.8) that that the spectral signal strength I_k, of the radiating species (k) for a transition ΔE_{ij} is a measure of the local number density N_k, $N_k \cdot \exp(\Delta E_{ij}/k_B T)$. Further, it is recalled that the Boltzmann plot of the number densities of the individual excited levels versus the corresponding energy levels yields a measure of the local electronic excitation temperature of the H atom. Additionally, the spectral broadening features of the atomic H lines can provide a measure of the electron number density of the plasma. The low resolution data of Figures 4.A and B are not suitable for these purposes, and very limited data were acquired using the higher resolution 1200 g/mm grating. The initial indications are that the sub-microsecond LIBS H_β data indicate electron density values on the order of $10^{17}/cm^3$.

Some of the first results of the H-lines LIBS testing, presented in Figure 1.13, are those describing the formation/decay of hydrogen lines (H_α, H_β, H_γ and H_δ n = 3, 4, 5, and 6) in the slightly fuel lean (F/O = Φ = 0.86) CH_4/O_2 laser plasma. These data were acquired from the onset of laser plasma to 5 μsec after. The line-width and intensity ratios of these H-lines provide information of LTE (local thermal equilibrium) and electron number density, as described by Eqn. 1.1 and/or 1.8.

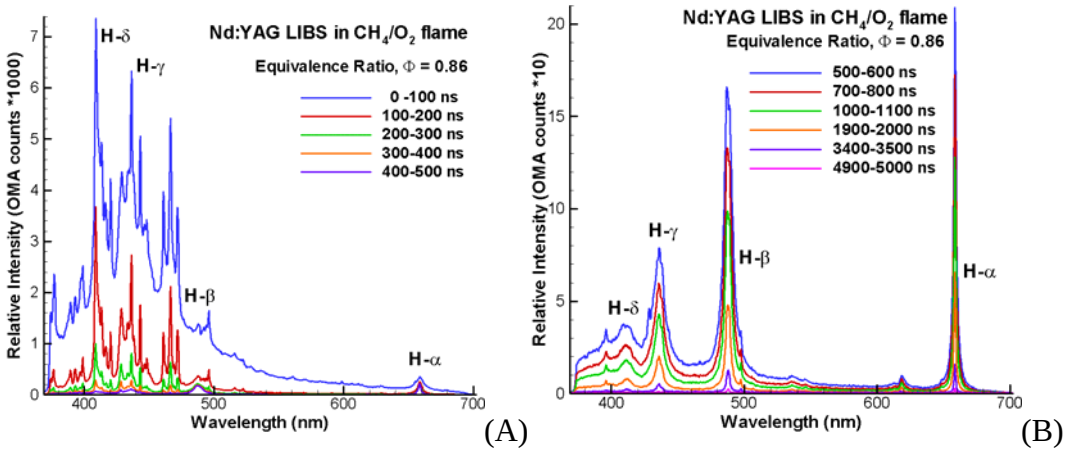

Figure 4. LIBS H-lines for Determination of LTE Condition and Electron (Plasma) Number Density

The attached results (Figure 5) show the survey spectra, in the UV region, for observation of C and O neutral and ionic atoms. The data were obtained in pure O_2 and CH_4 flows as shown and were obtained 100nsec after laser beam cessation and with a gate-width of 100nsec for data collection.

Single shot results at 100ns show strong C and O transitions in this region. The background noises are significant compared to the signals. At a later time of 250 ns following the breakdown, the carbon (^1S-$^1P^0$) line and oxygen iron (^2P-$^2D^0$) lines appear strong and free of interference in front of the decayed background. The signal-to-noise ratios for the 2 lines are superior. The 2-line C/O peak ratio can be used as the measurement metrics of the fuel/oxidant equivalence ratio. Shown in Figure 6 are the LIBS of the 2 selected lines performed in CH_4/O_2 flame for three equivalence ratios (Φ).

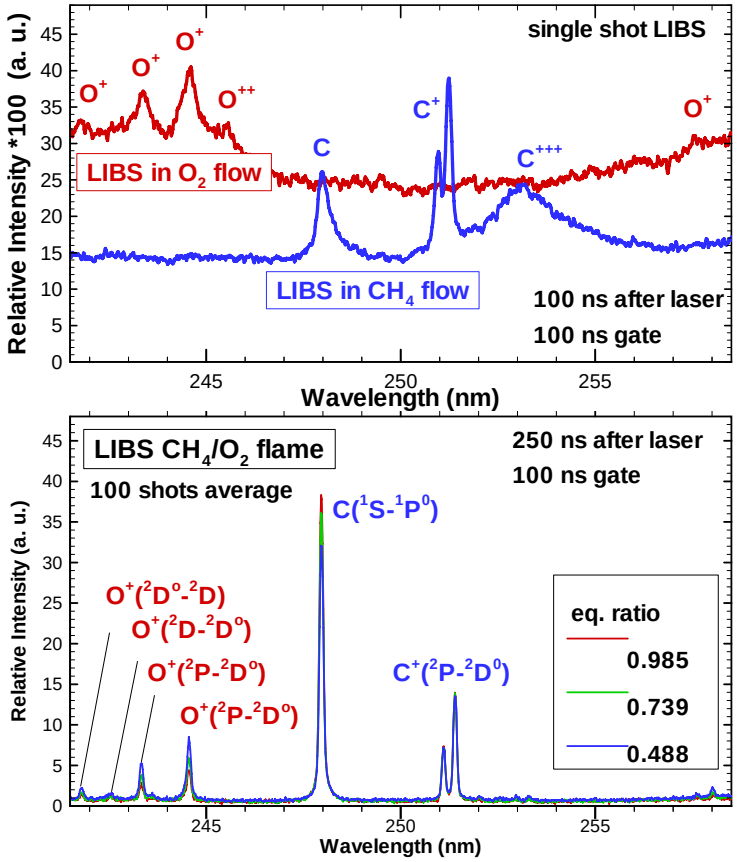

Figure 5. Survey Spectra of Carbon and Oxygen Neutral and Ionic Atoms in the UV Region

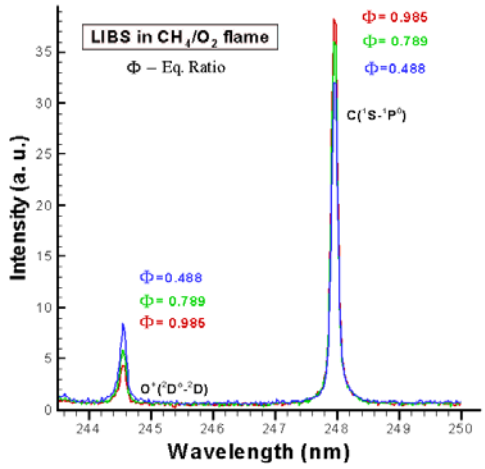

Figure 6. Survey Spectra of Methane and Oxygen in the UV Region for Three Equivalence Ratios (Flat Plate Burner)

The neutral C and the singly ionized O lines are the most attractive for use for the flame and are also applicable for the pure gas data as well. These data were obtained 250nsec after the laser pulse, and the clean background is to be noted. Also, the data in Figure 6 show clearly a variation of the signals with equivalence ratio. Further, the signal levels

observed scale reasonably well with expectations of the lower density flame region and the equivalence ratio variation. Again, single shot data can be obtained. Finally, Figure 7 shows the variation with equivalence ratio of the ratio of signals of C at 248nm and O^+ at 244.5nm (wavelength calibration is preliminary) that indicates feasibility of this method to determine C/O ratios.

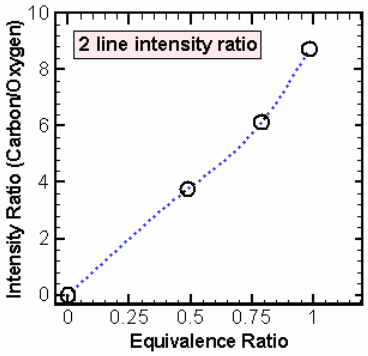

Eq. Ratio Validation

Pre-Set	LIBS Measurement
0.50	0.488
0.75	0.789
1.0	0.985

Figure 7. Equivalence Ratio From of Signals of C at 248nm and O^+ at 244.5nm (Wavelength calibration is preliminary)

Better and more accurate data were subsequently obtained at three different heights (4.5mm, 8mm, and 17mm) above the McKenna burner surface. These detecting locations sample different stages of the chemical reaction. Scanning through the laser plasma's decaying process we have located the best timing for strongest signals for both neutral carbon (^1S-$^1P^0$) line and oxygen iron (^2P-$^2D^0$) lines in CH_4/O_2 flame. Figure 8 shows the survey of the CH_4/O_2 flame of the McKenna burner for a set equivalence ratio of 0.5.

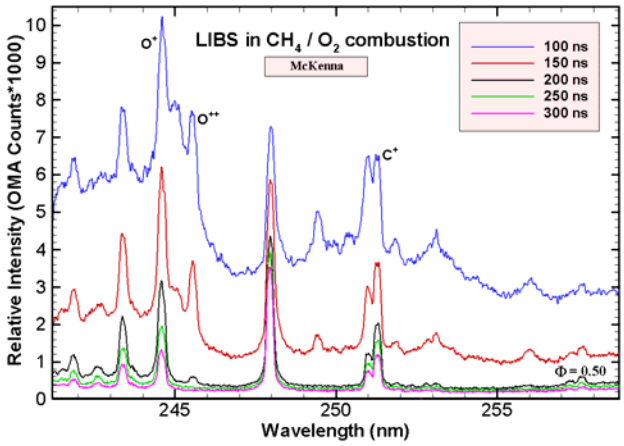

Figure 8. McKenna Calibration Tests. Determination of Optimal Delay Time from LIBS Survey using $\Phi = 0.5$ Methane/Oxygen Mixture

The best LIBS results were obtained with a delay time of approximately 200nsec. Thus, it was decided to use the LIBS with 200-ns delay time from laser breakdown for combustion with equivalence ratios between 0 and 2.0. The overall results in Figure 9 shows great confidence to the equivalence ratio (F/O) determination using the selected timing for the two selected lines (C and O^+) in UV region.

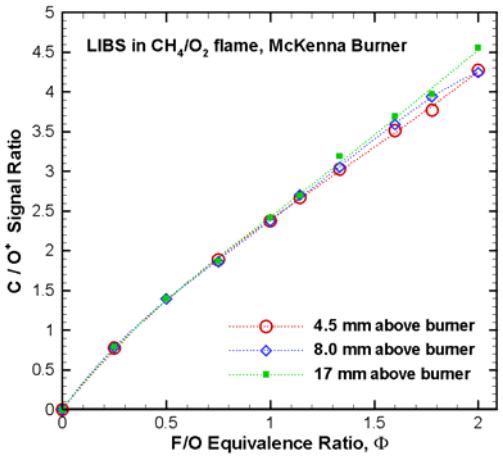

Figure 9. Final Calibration - Fuel to Oxidizer (F/O) Equivalence Ratio in CH_4/O_2 Flame From Flat Plate Burner (100-210nsec delay)

We also note that this calibration data, takes into account the pulse to pulse variation of the laser beam, the size of the laser induced spark (as discussed above), light absorption and optical loses. Based on these data, a good calibration curve for the equivalence ratio, Φ is:

$$\Phi = 0.502 \cdot \left(C/O^{+}\right) - 0.19 \qquad \text{Eqn. 1.9}$$

Finally, measurements 7mm above the McKenna burner were performed at various other chamber F/O ratios, 200 nsec delay and 100 ns gate, and the LIBS results were (consistently) in a good agreement with the experimentally measured equivalence ratios. Figure 10 is showing these results.

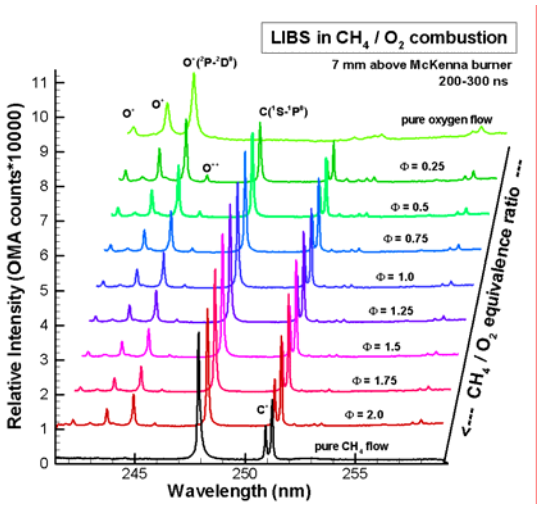

Figure 10. LIBS Measurements at Various Equivalence Ratios Covering the Entire Range From Pure Fuel (CH_4) Flow To Pure Oxidizer Flow (O_2)

Rocket Chamber LIBS Results

Following the flat plate calibration investigation, LIBS data was performed within the CFDRC rocket chamber. Figure 11 shows the chamber firing at UTSI and the laboratory LIBS instrumentation (as described in Figure 2)

Figure 11. Laboratory LIBS Rocket Chamber (A) and LIBS Instrumentation of Rocket Motor (B)

The LIBS results presented in Figure 12, were acquired within the rocket chamber at a pressure of 30psi (approx 2bar) and several delay times (of which only 3 are shown). The carbon (C) and O^+ peak ratio near 110-210 ns, $C/O^+ \cong 6$ indicates a condition of fuel rich, equivalence ratio of approximately 2.8 (as indicated by the calibration curve in Figure 9), which is higher than the set ratio which was approximately 1.5.-2.

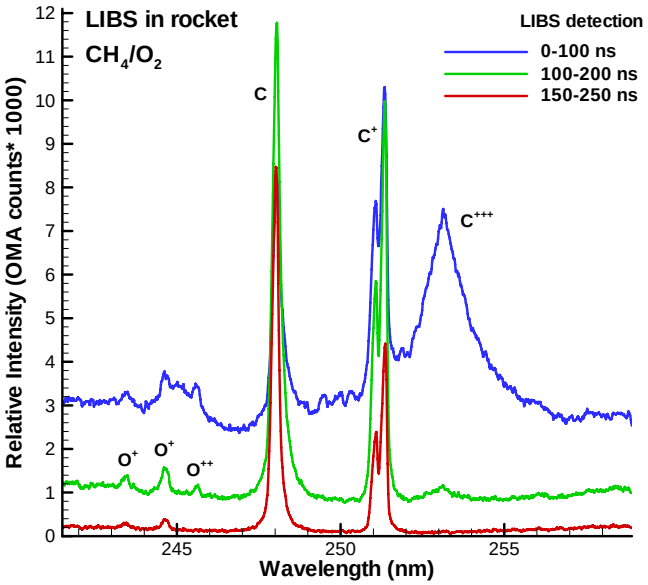

Figure 12. LIBS Results in Rocket Chamber. Measurements Indicating a Fuel Rich Breakdown Location

We believe that the spark breakdown measurements were performed at a location too close to the fuel inlet instead of a well-mixed region. Indeed, a subsequent CFD simulation of the chamber, see Figure 13, seems to corroborate the experimental results

by predicting regions (due to incomplete mixing) of high F/O ratio near the injector, where the measurements were performed.

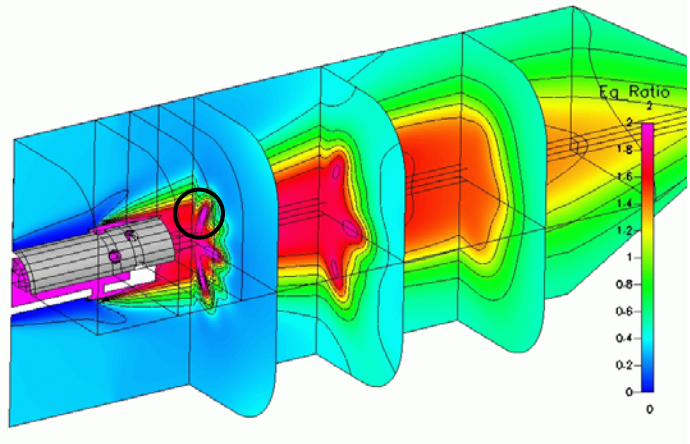

Figure 13. Local Values of Equivalence Ratio, as Computed by the CFD-ACE+ Flow Solver

Thus, one of the future goals of this program is to better determine the position of the breakdown and in the same time move the breakdown location close to the wall for better determination of the gas composition within the wall boundary layer. These measurements will then be used to validate results of CFD simulations for flow and heat transfer.

Wall Erosion and Health Monitoring

Health monitoring of the rocket chamber during combustion was demonstrated only qualitatively using spectroscopic monitoring of metal species in the ultraviolet/visible range of the spectrum. Since the rocket motor (and injector assembly) were manufactured from stainless steel 304 (Fe approx. 70%, Cr – 19%, Ni – 11% plus some trace Mn and Si), chamber/injector erosion was inferred from emission lines of these metals. Despite the poor resolution and sensitivity of the Ocean Optics HR 2000 spectrometer, utilized in Phase I, the recorded spectra in Figure 1.21 showed a consistent peak at 430 ±1nm associated with iron.

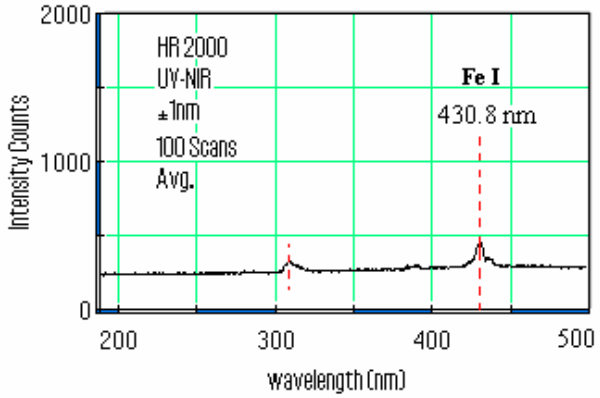

Figure 14. Iron Emission Line is a Candidate for LIBS Erosion Rate Determination

The NIST atomic emission wavelength database lists Fe I (430.79nm) as the only significant emission line at this wavelength. We concluded that the Fe I line is consistent with the observed burn-in of the injector assembly and with the high concentration of iron in the SS304. The tests have also shown that in the UV (200-350nm) range the integrated background emission is virtually zero. Similar tests were run also at UTSI using a gated spectrometer of higher resolution (±0.01nm). Though engine operation was limited by extreme thermal heating of the combustion chamber, we have obtained the most critical data for LIBS under combustion conditions. This laboratory provides conclusive evidence that the LIBS signal levels are adequate for this purpose.

Engine health monitoring will focus on detecting and quantifying the presence of multiple metallic species (Fe, Cu, Cr, Mn, etc.,) in the combustion volume using spectroscopic investigation of the light emitted by the post breakdown plasma. These tests will feature a sacrificial rod, which will be introduced into the combustion chamber and will release the metallic species of choice into the combustion mixture at a known rate. The ablation rate of the rod will be measured after each test by weighting and will provide the calibration data for the LIBS measurement.

Increased Pressure LIBS Measurements

The use of LIBS at the increased pressures associated with rocket combustion is promising because laser breakdown of gases and two-phase mixtures can be achieved with greater ease at increased pressures than for the lower pressure environments. As with lower pressures the atomic and ionic spectral lines occur following the laser pulse, during the temporal period of the plasma for which local thermal equilibrium has been attained, and prior to the characteristic time of formation of molecules.

There are, however, some challenges in the application of LIBS within high-pressure and -density combustors. One of these difficulties is the large continuum background radiation of the plasma. It's helpful to recall that a 30,000K plasma would have a blackbody spectrum that peaks near 100 nm and that our measurements are typically in the 200-400 nm spectral region. As the atomic line radiation emerges from the sea of background radiation, the signal-background ratio is determinative of the goodness of the measurement. A second important aspect of LIBS in this density range is the time-dependence of the atomic-ionic spectral signals. Monotonic decay rates are desired, and the decay times must be sufficiently great to allow measurements after decay of the large background signals. Measurements are underway to define these parameters in the determination of mixture ratio for increased pressure applications. Preliminary results of LIBS spectra of carbon dioxide are shown in Figure 15. These data show specific atomic and ionic carbon line spectra for CO2 over the pressure range of 0.1 – 3 atm. The ability to determine neutral and ionic carbon signals is also shown. From these and other data, the potential to utilize LIBS to ascertain mixture ratio continues to appear feasible at the pressure levels found in rocket combustion applications.

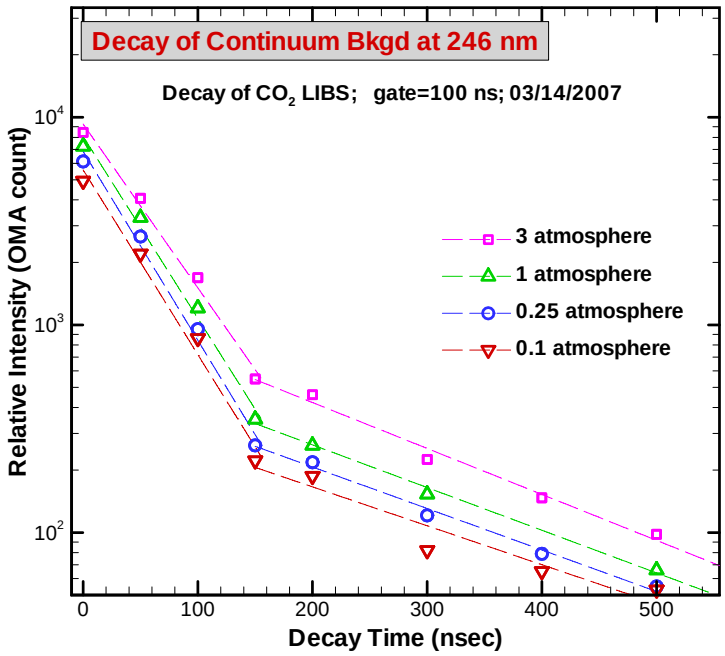

a) Influence of pressure on continuum radiation level and decay rate

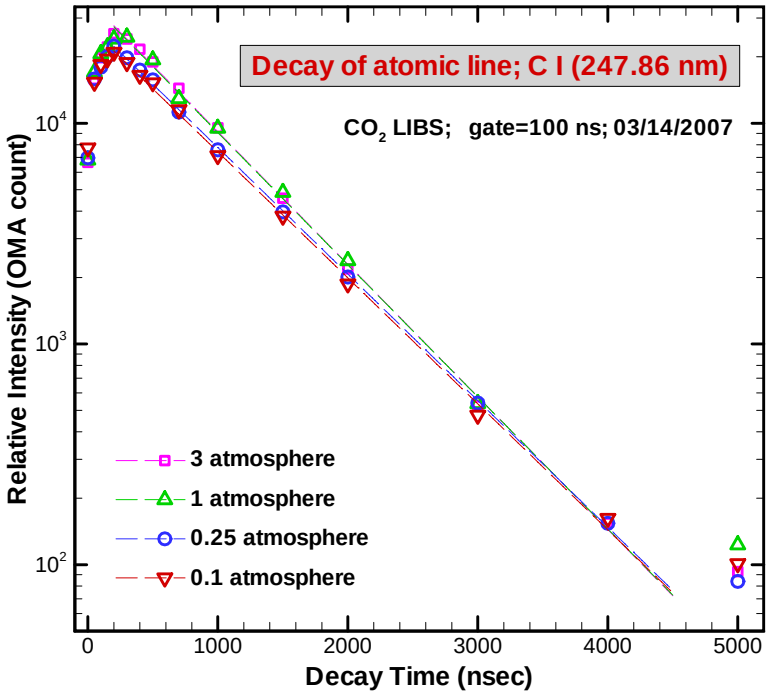

b) Influence of gas pressure on signal level and decay rate

Figure 15. Gas pressure may have minimal influence on atomic spectral line signal level and decay rate.

Conclusions

LIBS measurements of the equivalence ratio in methane-oxygen flames at atmospheric pressure as well as within a rocket motor at 2bar were performed and the experimental data showed fairly consistent and reproducible results. The equivalence ratio measured within the rocket motor was somewhat (approximately 50%) higher that the average equivalence ratio set for the motor. It is assumed that the location of the laser spark in a region of higher methane concentration was responsible for the result. Future tests will need to be run to assert this with a higher degree of confidence. Repeated measurements were made of the background signals in the spectral vicinity of the previously selected C and O^+ transitions. The results showed that background signals are negligible for gate-widths that will be used during LIBS measurements in the UV range. Also, estimates of the transmission factor of the optical fiber indicate attenuation of the anticipated signal to be acceptable.

References

Anglos, D. et al, Laser Diagnostics of Painted Artworks: Laser Induced Breakdown Spectroscopy in Pigment Identification, Applied Spectroscopy, Vol. 51, No. 7, pp. 1025-1030, 1997.

Chen, Y.L., Ph. D Dissertation, UTSI 1998.

Chen, Y. L., Lewis, J. W. L., and Parriger, C., Spatial and temporal profiles of pulsed laser-induced air plasma emissions, Journal of Quantitative Spectroscopy & Radiative Transfer, Vol. 67, pp. 91-103, 2000.

Dors, I. Ph.D Dissertation, UTSI 2000.

Fang, Y. Y., Sharma, R. C., Singh, J. P., Zhang, H., and Spencer, W. A., Evaluation of the Potential of Laser Induced Breakdown Spectroscopy for the Detection of Trace Element in Liquid, J. Air and Waste Manage. Assoc., Vol. 52, pp1307-1315, Nov 2002.

Ferioli, F. et al., Laser-Induced Breakdown Spectroscopy for Online Engine Equivalence Ratio Measurements, Applied Spectroscopy, Vol. 57, No. 9, pp. 1183-1189, 2003.

Fisher, B. et al, T., Temporal Gating for the Optimization of Laser Induced Breakdown Spectroscopy Detection and Analysis of Toxic Metals, Applied Spectroscopy, Vo. 55, Number 10, pp. 1312-1319, 2001.

Hohreiter, V. Hahn, D. W., Dual-Pulse Laser Induced Breakdown Spectroscopy: Time-resolved Transmission and Spectral Measurements, Spectrochimica Acta Part B, Vol. 60, pp. 968-974, 2005.

Phuoc, X.T., White, F., Laser-induced spark ignition of CH4–air mixtures, Combust. Flame 119, pp. 203–216, 1999.

Plemmons, D. H. Ph.D Dissertation, The University of Tennessee Space Institute, 1996.

Sandrowitz A. K., at al. Flame Emission Spectroscopy for Equivalence Ratio Monitoring, Applied Spectroscopy, Vol. 52, No. 5, pp. 658-662, 1998.

Laser Induced Breakdown Spectroscopy (LIBS) Applied to Reacting Gases for Mixture Ratio Measurement and Detection of Metallic Species

Matthew Thomas
Stelu Deaconu
CFD Research Corporation
Jim Lewis
University of Tennessee Space Institute
Edward Coy
Air Force Research Laboratory

54th. JANNAF JPC Conference
May 14 – 17, 2007

Introduction

- LIBS has been applied to a variety of applications in research but a limited number of industrial applications. It has yet to be successfully examined as a combustion diagnostics and health monitoring approach within the interior of a rocket combustion chamber.

- Virtually all of the LIBS work within the combustion chamber is still qualitative due to the complexity of the plasma plume and its impact on quantitative LIBS measurements.

- The combined research and development effort being pursued here will examine the potential of LIBS within the high pressure combustion environments in a rocket thrust chamber.

Background

- **Laser Induced Breakdown Spectroscopy (LIBS) is an optical diagnostic technique capable of providing an analysis of the local concentration of various atomic species.**
- **LIBS uses a single or double pulse laser beam to produce a plasma within the focal region that includes the test point, and is applicable to single-, two-, and multi-phase media.**

HOW?

Use These Equations and Calibration Data!

Spectrally Integrated Line Intensity

$$\frac{I_\alpha(T_\alpha)}{I_r(T_r)} = \frac{C_\alpha}{C_r} \cdot \frac{\exp\left(-E_k/k_B\left(1/T_\alpha - 1/T_r\right)\right)}{U_\alpha(T_\alpha)/U_r(T_r)}$$

Broglie Wavelength

$$\Lambda \cong \sqrt{\frac{h^2}{2\pi \cdot m_e k_B T}}$$

Saha Equation

$$\frac{n_i + n_e}{n_i} = \frac{2}{\Lambda^3} \cdot \frac{g_{i+1}}{g_i} \exp\left[-\frac{\left(\varepsilon_{i+1} - \varepsilon_i\right)}{k_B T}\right]$$

Plasma Temperature Determination

$$I(\upsilon) = \frac{2h\upsilon^3}{c^2} \cdot \frac{1}{\exp(h\upsilon/kT) - 1}$$

Plasma Temperature Estimation

$$\ln\left(\frac{I_\alpha}{g_k \cdot A_{ki}}\right) = -\frac{E_k}{k_B \cdot T} + \ln\left(\frac{C_\alpha \cdot \beta}{U_\alpha(T_\alpha)}\right)$$

Spontaneous Emission

$$n(t) = n_0 \cdot e^{-t \cdot A_{21}}$$

Species Determination

$$I_\alpha = \beta \cdot C_\alpha \frac{g_k A_{ki} \cdot \exp\left(-E_k/k_B T\right)}{U_\alpha(T)}$$

Species Concentration

$$I_{ij} = \alpha \cdot N_k \cdot A_{ij} \cdot \exp\left(-\Delta E_{ij}/k_B T\right)$$

Technical Approach

- Flat Flame LIBS Calibration for GOX/CH4
- Fabrication of Test Rocket Motors
- Low Pressure LIBS Measurements in Rocket Chamber
- Detection of Metallic Species

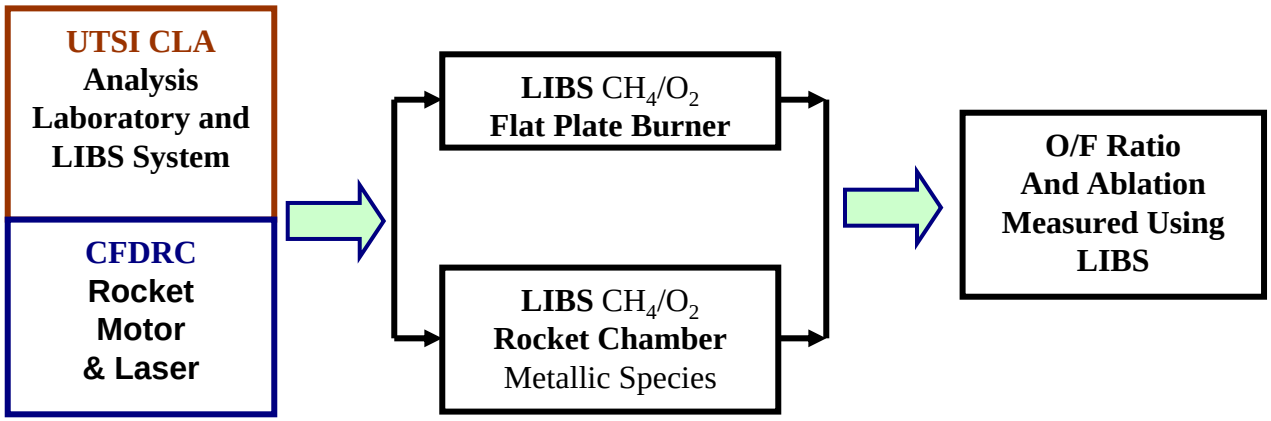

Laboratory LIBS Setup

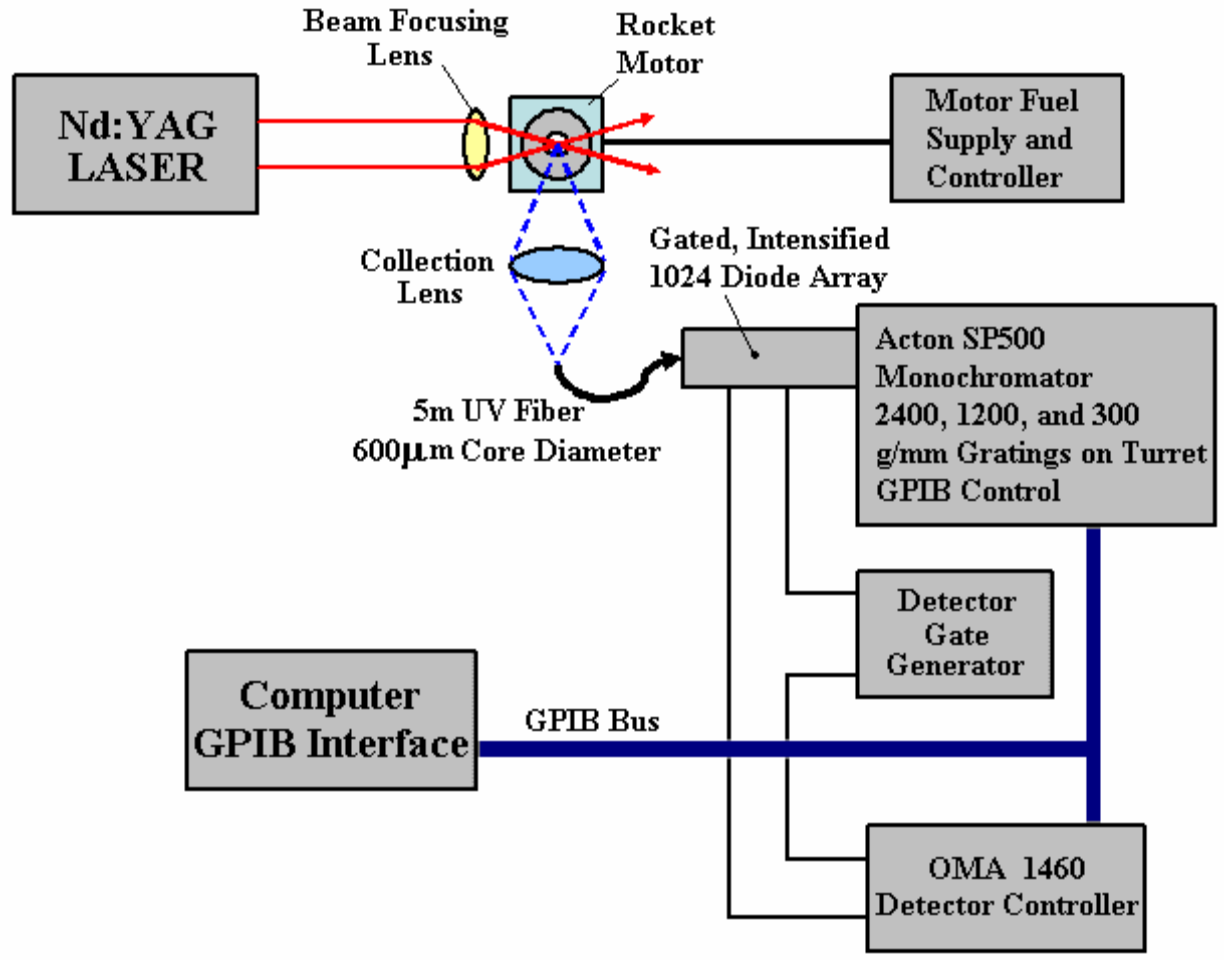

LIBS Instrumentation and Hardware

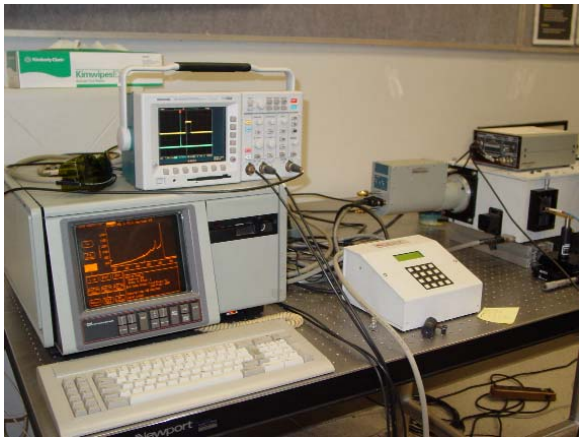

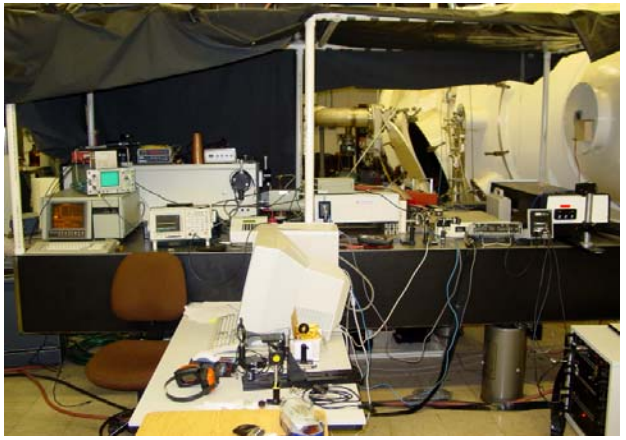

UTSI Test Apparatus

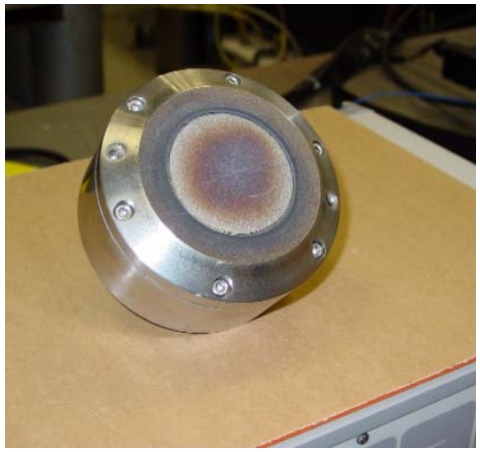

Mekenna Bruner

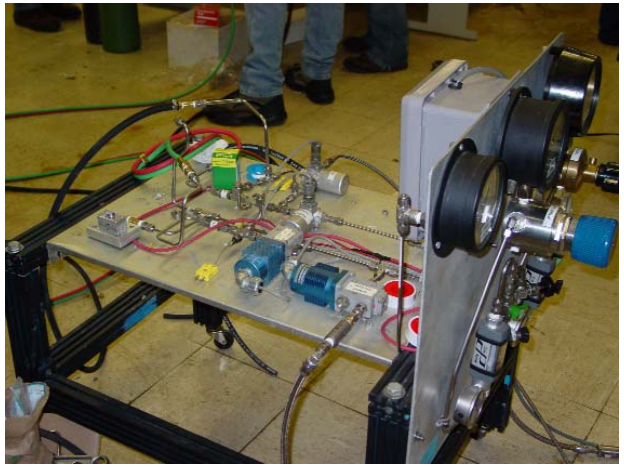

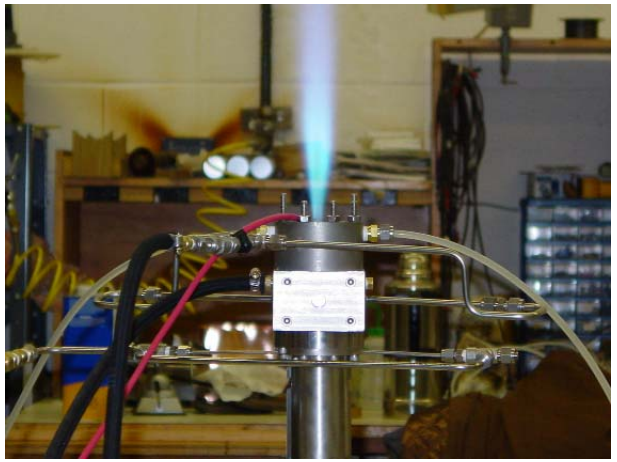

Rocket Chamber

Flat Flame Calibration Testing

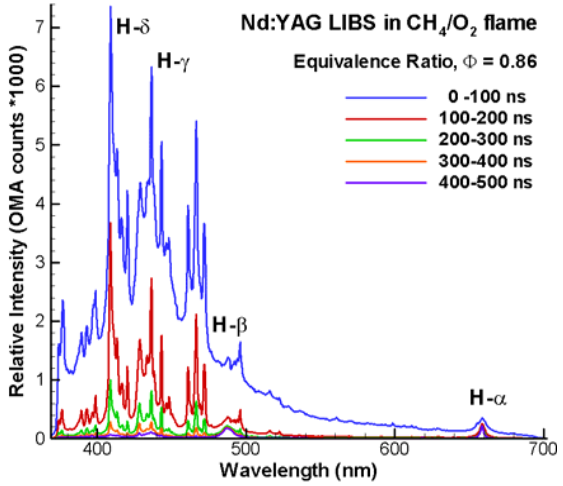

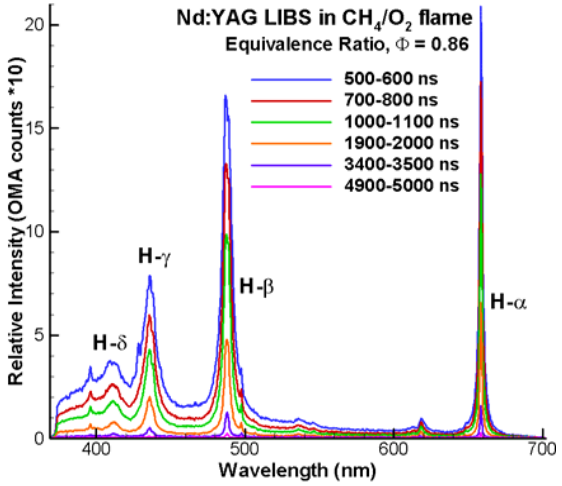

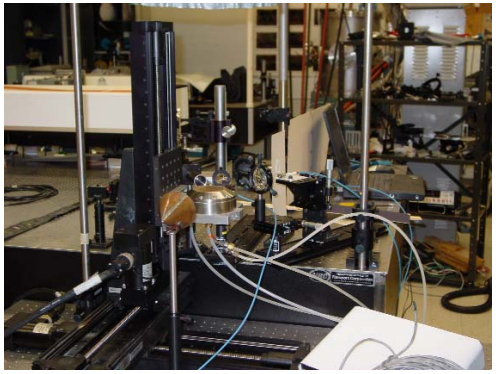

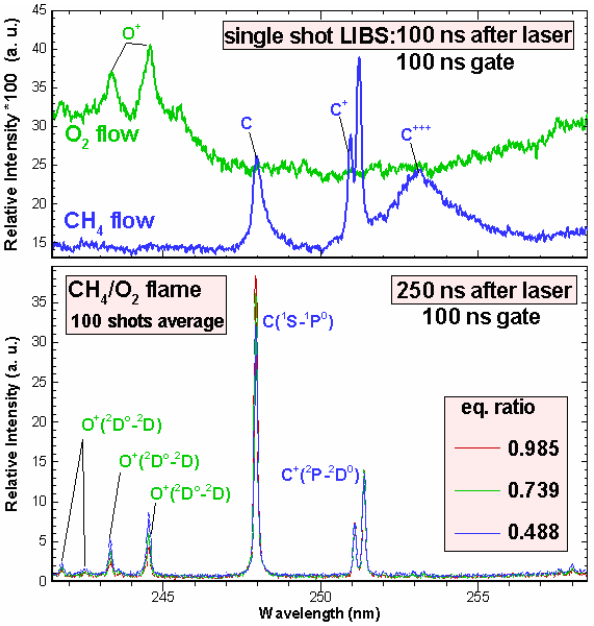

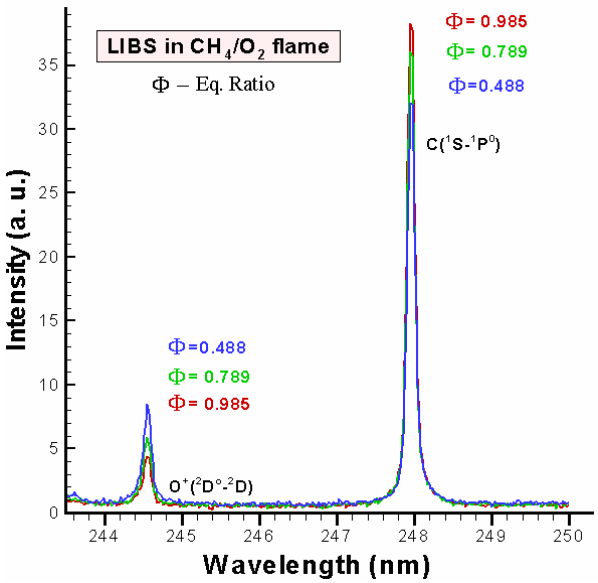

O/F Ratio Calibration Curve

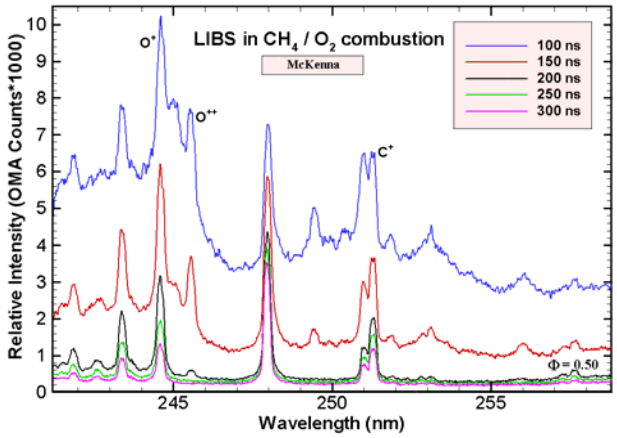

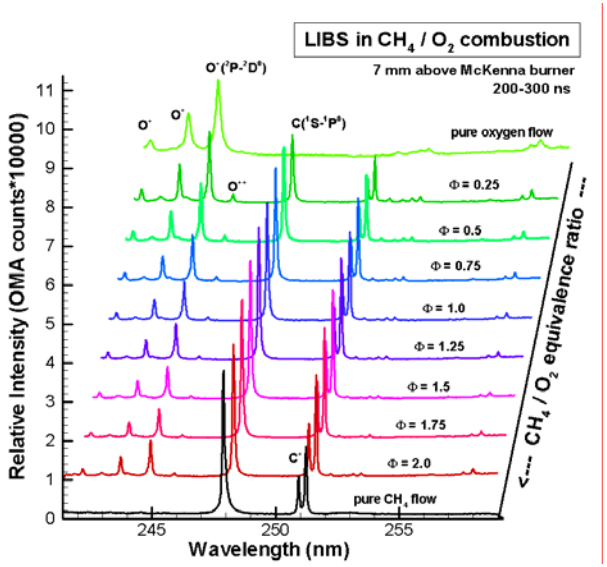

$$\Phi = 0.502 \cdot \left(C/O^{+}\right) - 0.19$$

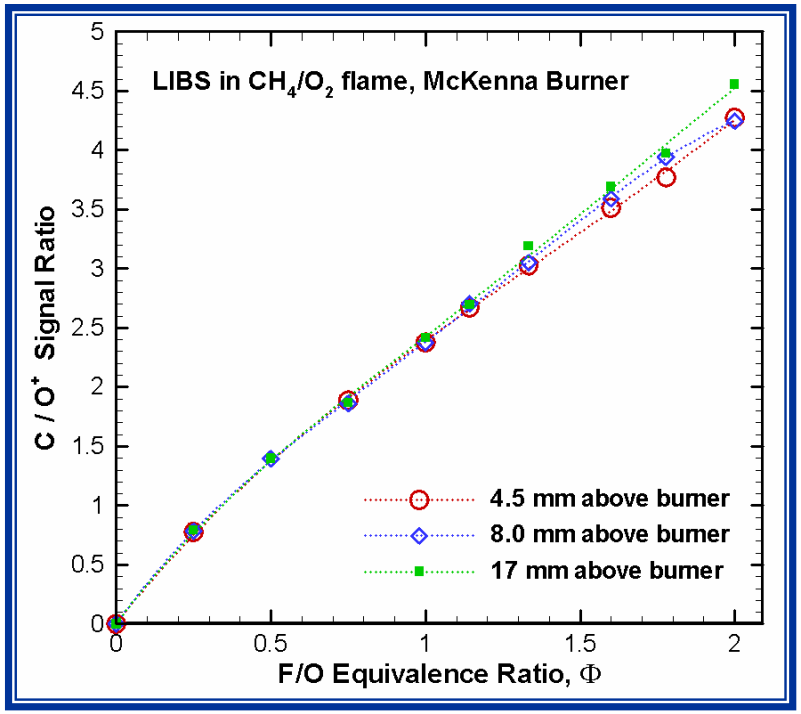

Equivalence Ratio vs. C/O⁺ Signal From Flat Flame LIBS Data

Two Test Motors

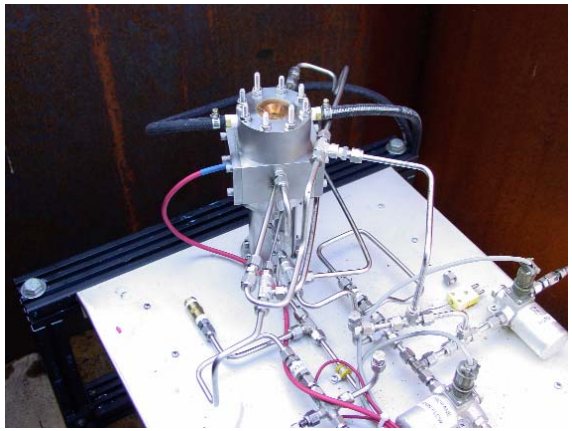
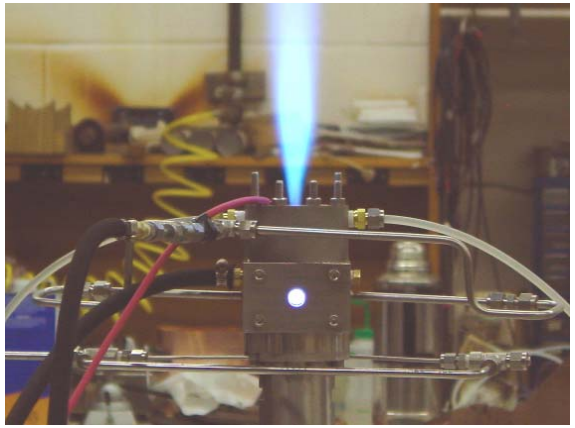
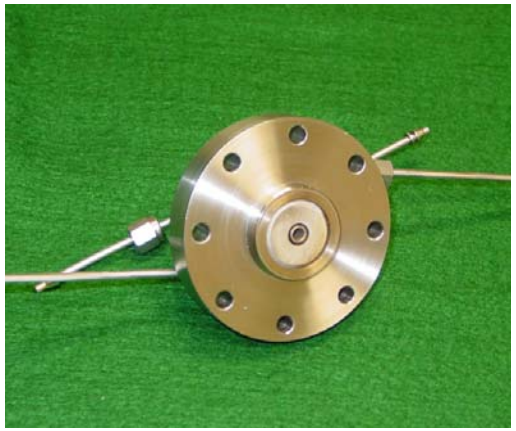

Water Cooled Nozzle with Swirl Coax Element

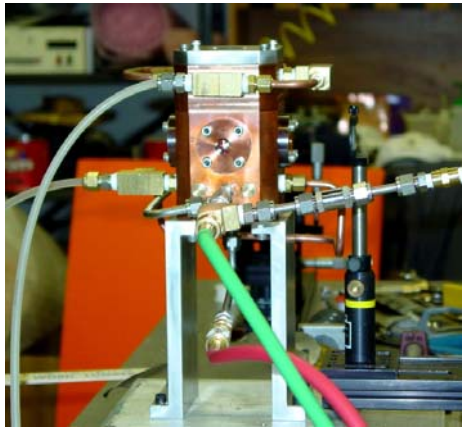
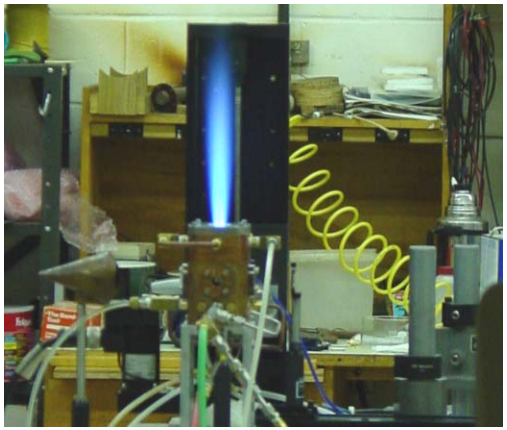


Water Cooled Chamber with Impinging Injector

Low Pressure (30psia) LIBS Rocket Data

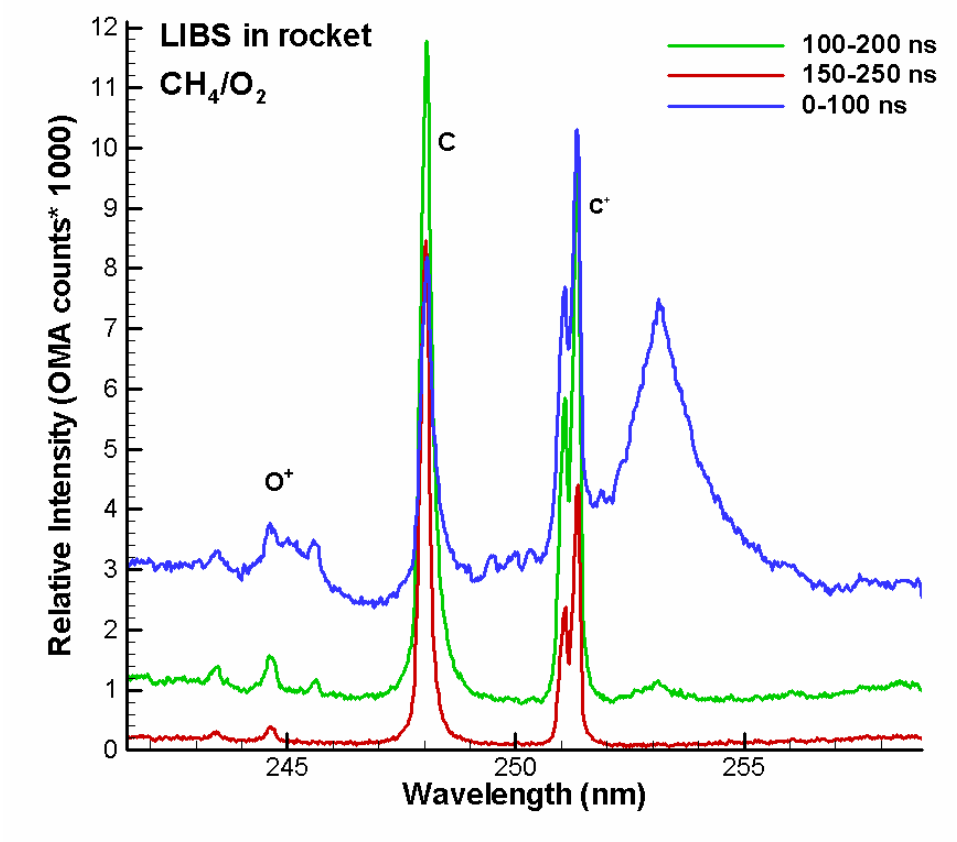

The carbon (C) and O^+ peak ratio using 100-200nS gating indicates an equivalence ratio > 4.0

A preliminary CFD prediction of 2.8 was observed for the identical location.

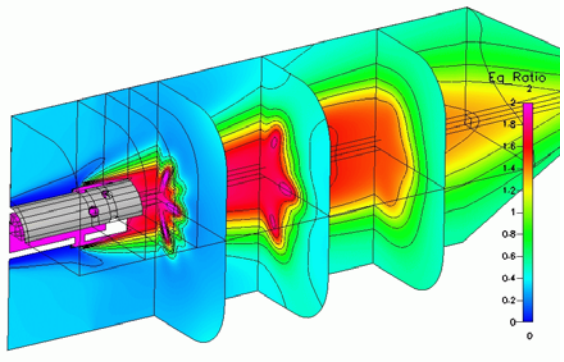

Detection of Metallic Species

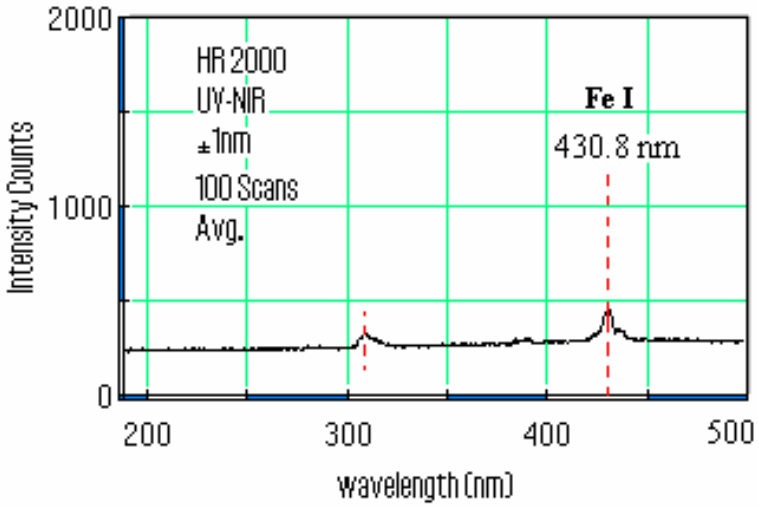

Spectroscopic measurements in the combustion zone indicate the presence of Fe I atomic line.

Ablation of the injector stem during testing corroborated this observation.

- Data was insufficient to estimate ablation rate.

Future Efforts

- Generate LIBS Calibration and Operational Procedures for Rocket Combustion and Health Monitoring
- Demonstrate Fiber Optic Coupled/LIBS System Operation in a Bipropellant Rocket Combustion Chamber (LOX/CH4, GOX/CH4) at high pressure.

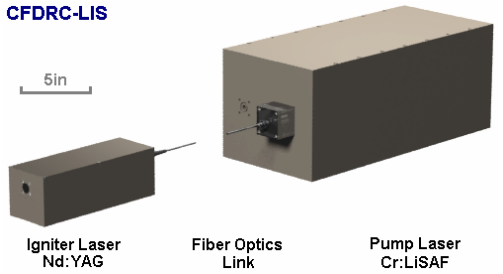

- Perform near-wall LIBS measurements to support ongoing validation of heat transfer predictions from CFD Codes.
- Demonstrate LIBS Measurements using a Single Optical Access Window.

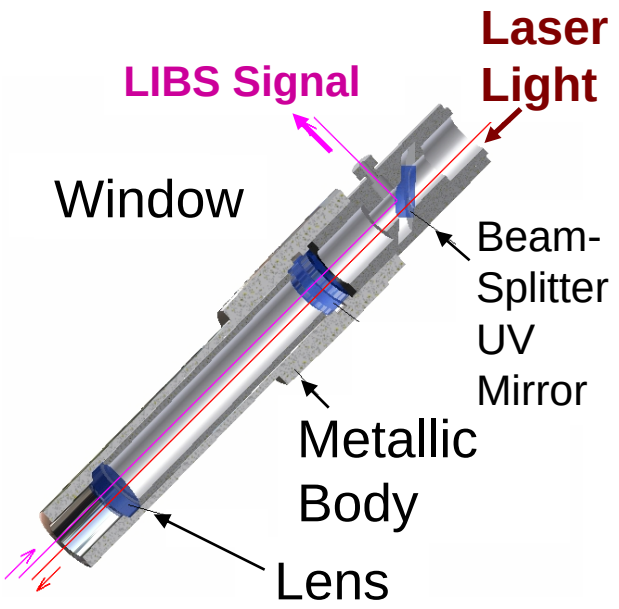

Conclusions

- **LIBS measurements of the equivalence ratio and metal erosion associated with methane-oxygen flames in a MeKenna burner and a rocket motor were successfully completed.**
- **Equivalence ratio measurement up to 4.0 is feasible.**
- **Future tests will need to be run to assert this with a higher degree of confidence.**
- **The results showed that background signals are negligible for gate-widths that will be used during LIBS measurements in the UV range.**
- **Estimates of the transmission factor of the optical fiber indicate attenuation of the anticipated signal to be acceptable.**